

A potential suite of climate markers of long-chain n-alkanes and alkenones preserved in the top sediments from the Pacific sector of the Southern Ocean

Xin Chen (✉ chenxust@mail.ustc.edu.cn)

Xiaodong Liu

China University of Science and Technology

Da-Cheng Lin

National Taiwan Ocean University

Jianjun Wang

Third Institute of Oceanography SOA

Liqi Chen

Third Institute of Oceanography SOA

Pai-Sen Yu

Taiwan Ocean Research Institute

Linmiao Wang

First Institute of Oceanography

Zhifang Xiong

First Institute of Oceanography

Min-Te Chen

National Taiwan Ocean University

Research article

Keywords: Southern Ocean, Pacific Ocean, n-alkane, carbon isotopic, SST, U37k

Posted Date: January 6th, 2021

DOI: <https://doi.org/10.21203/rs.3.rs-51878/v2>

License:  This work is licensed under a Creative Commons Attribution 4.0 International License.

[Read Full License](#)

Version of Record: A version of this preprint was published at Progress in Earth and Planetary Science on April 6th, 2021. See the published version at <https://doi.org/10.1186/s40645-021-00416-9>.

A potential suite of climate markers of long-chain *n*-alkanes and alkenones preserved in the top sediments from the Pacific sector of the Southern Ocean

Xin Chen^{1,3*}, Xiaodong Liu¹, Da-Cheng Lin², Jianjun Wang³, Liqi Chen³, Pai-Sen Yu⁴,
Linmiao Wang⁵, Zhifang Xiong⁵, Min-Te Chen^{2,6*}

¹ Anhui Province Key Laboratory of Polar Environment and Global Change, School of Earth and Space Sciences, University of Science and Technology of China, Hefei, Anhui 230026, China

² Institute of Earth Sciences & Center of Excellence for the Oceans & Center of Excellence for Ocean Engineering, National Taiwan Ocean University, Keelung, 20224, Taiwan

³ Key Laboratory of Global Change and Marine - Atmospheric Chemistry (GCMAC) of Ministry of Natural Resources (MNR), Third Institute of Oceanography (TIO), MNR, Xiamen 361005, China

⁴ Taiwan Ocean Research Institute, National Applied Research Laboratories, Kaohsiung 80143, Taiwan

⁵ Key Laboratory of Marine Geology and Metallogeny, First Institute of Oceanography, Ministry of Natural Resources, Qingdao 266061, China

⁶ Pilot National Laboratory for Marine Science and Technology, Qingdao 266061, China

*Corresponding author: Xin Chen (chenxust@mail.ustc.edu.cn) and Min-Te Chen (mtchen@mail.ntou.edu.tw)

Abstract

Investigating organic compounds in marine sediments can potentially unlock a wealth of new information in these climate archives. Here we present pilot study results of organic geochemical features of long-chain *n*-alkanes and alkenones and individual carbon isotope ratios of long-chain *n*-alkanes from a newly collected, approximately 8-meter long, located in the far reaches of the Pacific sector of the Southern Ocean. We analyzed a suite of organic compounds in the core. The results show abundant long-chain *n*-alkanes (C₂₉-C₃₅) with predominant odd-over-even carbon preference, suggesting an origin of terrestrial higher plant waxes via long-range transport of dust, possibly from Australia and New Zealand. The $\delta^{13}\text{C}$ values of the C₃₁ *n*-alkane range from -29.4 to -24.8‰, in which the higher $\delta^{13}\text{C}$ values suggest more contributions from C₄ plant waxes. In the analysis, we found that the mid-chain *n*-alkanes (C₂₃-C₂₅) have a small odd-over-even carbon preference, indicating that they were derived from marine non-diatom pelagic phytoplankton and microalgae and terrestrial sources. Furthermore, the C₂₆ and C₂₈ with lower $\delta^{13}\text{C}$ values (\sim -34‰) indicate an origin from marine chemoautotrophic bacteria. We found that the abundances of tetra-unsaturated alkenones (C_{37:4}) in this Southern Ocean sediment core ranges from 11-37%, perhaps a marker of low sea surface temperature (SST). The results of this study strongly indicate that the $\delta^{13}\text{C}$ values of long-chain *n*-alkanes and U₃₇^k index are potentially useful to reconstruct the detailed history of C₃/C₄ plants and SST change in the higher latitudes of the Southern Ocean.

Keywords: Southern Ocean; Pacific Ocean; *n*-alkane; carbon isotopic; SST; U_{37}^k

1 **1. Introduction**

2
3 The Southern Ocean plays an important role in global climate and the carbon cycle related to westerly
4 winds and the Antarctic Circumpolar Current (ACC, Fischer et al. 2010; Marshall and Speer 2012).
5 Mid-latitude westerly winds are essential in transporting mineral dust from the continent of Australia and
6 New Zealand to the South Pacific sector of the Southern Ocean (Lamy et al. 2014). The westerly winds
7 and ACC's location and intensity directly control the exchange of heat, salt, nutrients, and freshwater
8 between low and high latitudes (Pahnke and Zahn 2005; Toggweiler and Russell 2008; Shevenell et al.
9 2011; Toyos et al. 2020). Thus, environmental fluctuations in the Southern Ocean play a vital role in global
10 climate change.

11 Well preserved organic matter in marine sediments is a direct indicator of environmental conditions at
12 the time of sedimentation and thus is important for paleo-environmental studies (Meyers and Ishiwatari
13 1993). Among these, lipid organic biomarkers have been widely used to reconstruct past environmental
14 and climatic conditions in oceans and lakes (Eglinton and Eglinton 2008; Holtvoeth et al. 2019).
15 Long-chain *n*-alkanes (C₂₅-C₃₅) are important components of the epicuticular wax in higher terrestrial
16 plants, and these *n*-alkanes are eroded from leaf surfaces and soil by winds and then transported to the
17 Southern Ocean (Bendle et al. 2007; Martínez-García et al. 2009, 2011; Lamy et al. 2014; Jaeschke et al.
18 2017). Short- and mid-chain lengths are the major components of *n*-alkanes in the surface ocean sediments
19 around Antarctica. These compounds mainly derived from phytoplankton and bacteria based on carbon
20 preference index (CPI) and specific-compound carbon isotopic values (Harada et al. 1995; Bubba et al.
21 2004). Relatively higher carbon isotopic values of C₃₁ *n*-alkane in the surface sediments from the
22 Australian sector of the Southern Ocean suggest significant contributions of C₄ higher vascular plant
23 waxes or conifer resin (Ohkouchi et al. 2000). Altered or recycled material mixed with modern marine
24 input is also an important source for long-chain *n*-alkanes with low CPI values in ocean sediments in the
25 Ross Sea region (Kvenvolden et al. 1987; Venkatesan 1988; Duncan et al. 2019). Although the high
26 latitudes of the Southern Ocean are usually considered to be little influenced by river and continent soils,
27 based on the above results, the sources of *n*-alkanes in the ocean sediments are thought to be complicated;
28 thus their eco-environmental implications are still being explored.

29 Subtropical to polar sea surface temperature (SST) gradient has been related to the position and
30 intensity of the westerly winds and ACC in the Southern Ocean (Lamy et al. 2010; Kohfeld et al. 2013).
31 Therefore, quantitative SST records from the past are essential for evaluating the importance of the
32 Southern Ocean for the global climate. However, the most widely used organic geochemical SST index,
33 alkenone paleothermometry, has only rarely been employed in high latitudes of the Southern Ocean. The

34 $U_{37}^k = ([C_{37:2} - C_{37:4}] / [C_{37:2} + C_{37:3} + C_{37:4}])$ index has been proposed to quantify the degree of alkenone
35 unsaturation (Brassell et al. 1986), which is a function of SST. Because $C_{37:4}$ is often absent in open ocean
36 sediments when SSTs are higher than 12°C (Prah and Wakeham 1987), the index was simplified to $U_{37}^{k'} =$
37 $([C_{37:2}] / [C_{37:2} + C_{37:3}])$. In recent decades, the $U_{37}^{k'}$ index has been widely used in middle and low latitude
38 marine environments. However, our knowledge on the application of alkenone paleothermometry in the
39 high latitudes of the Southern Ocean is still largely insufficient. A few examples exist, such as that $C_{37:4}$
40 methyl alkenone was not detected in the 10-12°C waters. Even in the 1.5°C waters, the abundance was still
41 very minor (Sikes and Volkman 1993), while it was detected in most surface sediment samples at 3.5°C in
42 spring cruise samples in the Southern Ocean (Sikes et al. 1997). The relative abundance of $C_{37:4}$ alkenone
43 in the surface sediments showed no significant relationship with modern SST, suggesting that the $U_{37}^{k'}$
44 index may be more proper than U_{37}^k when used in sea surface temperature estimations, even in cold
45 conditions (Sikes et al. 1997; Jaeschke et al. 2017). However, Ho et al. (2012) found that the U_{37}^k records
46 display better agreement with planktic foraminifera $\delta^{18}O$ and other SST records at the same sites,
47 suggesting the U_{37}^k is more suitable for SST reconstructions in the subantarctic Pacific. Data on alkenone
48 paleothermometry is still largely lacking and these various results of U_{37}^k and $U_{37}^{k'}$ -SSTs indicate that
49 more investigations are still needed in the high latitudes of the Southern Ocean.

50 Considering the importance of the position and strength of westerly winds and the Antarctic
51 Circumpolar Current, reconstructing surface ocean hydroclimatic changes using organic biomarkers (e.g.,
52 long-chain *n*-alkanes and alkenones) is necessary to better understand the role of the Southern Ocean in the
53 context of global climate change. Before carrying out such work, it is crucial to determine the source of
54 organic matter and to estimate whether the U_{37}^k index could be useful or not in the Southern Ocean. Here,
55 we analyze the organic geochemical features of long-chain *n*-alkanes, alkenones, and the
56 compound-specific carbon isotope of long-chain *n*-alkanes (C_{23} - C_{31}) in the ocean sediments from one core
57 in the South Pacific sector of the Southern Ocean (R23, 66°13'47.16"S, 168°11'8.34"E). Our main
58 objectives are: (a) to evaluate the source of long-chain *n*-alkanes based on their chain length distributions
59 and individual carbon isotopes, (b) to report the distributional features of di-, tri- and tetra-unsaturated
60 alkenone, and (c) to assess the applicability of the alkenones indices in the high latitudes of the Southern
61 Ocean for reconstructing past climate changes.

62 63 **2. Materials and methods**

64 65 **2.1 Materials**

66

67 The gravity core R23 was drilled at 168°11'8.34"E, 66°13'47.16"S at a water depth of 2967 m during
68 the "31th Chinese National Antarctic Research Expedition (CHINARE)" cruise in 2014-2015 (Fig. 1). The
69 sediment core is 819 cm long, with a top 10 cm soupy layer characterized by high water content. The core
70 was subsampled at an interval of 2 cm. The color of the sediments varies among olive, brown and gray
71 throughout the profile. Based on the wet and dry sieving experiments, the core mainly consists of
72 homogenous clay with minor proportions of sand (63-2000 μm), some ice-rafted debris (IRD; >2 mm) and
73 some foraminifera are randomly found, but sponge spicules are present throughout the core with relatively
74 high abundance. No obvious bioturbations were observed in this core. In this pilot study, we only focus on
75 the source identification of *n*-alkanes with different chain lengths and then evaluate the possibility of C_{37}
76 alkenones used as a suitable proxy for calculating the past sea surface temperature in this region. To study
77 the potential of sedimentary organic geochemical features for paleoclimate reconstruction, we choose 12
78 samples at every ~ 80 cm interval for *n*-alkanes and alkenones analysis in this pilot study. All samples
79 were stored under -20°C in the lab before analysis.

80

81 2.2 Lipids biomarker extraction

82

83 The lipids analysis procedure followed the methods of Yamamoto et al. (2000). Briefly, all sediment
84 samples were freeze-dried and then homogenized and powdered. Samples (2-3 g) were weighed, and
85 extracted two times with an Accelerated Solvent Extractor (DIONEX ASE 350) using
86 dichloromethane-methanol (6:4 v/v) and then concentrated. The total lipid extract was separated into four
87 fractions using column chromatography (SiO_2 with 5% distilled water; internal diameter, 5.5 mm; length,
88 45 mm) based on the degree of polarity: F1 (hydrocarbons, 4 ml hexane); F2 (aromatic hydrocarbons, 4 ml
89 hexane-toluene (3:1 v/v)); F3 (ketones, 4 ml toluene); F4 (polar compounds, 4 ml toluene-methanol (3:1
90 v/v)). $\text{N-C}_{24}\text{D}_{50}$ and $\text{n-C}_{36}\text{H}_{74}$ were added as internal standards for the F1 and F3 fraction, respectively.
91 Compounds were quantified using an internal standard $\text{n-C}_{24}\text{D}_{50}$ and $\text{n-C}_{36}\text{H}_{74}$ for *n*-alkanes and alkenones,
92 respectively.

93

94 2.3 *n*-alkanes and alkenones analysis

95

96 Quantification of compounds was performed on a Hewlett Packard 6890 GC-FID system with a
97 Chrompack DB-1MS column (length, 60 m; i.d., 0.25 mm; thickness, 0.25 μm). The oven temperature was
98 programmed from 70 to 290°C at 20°C/min, 290 to 310°C at 0.5°C/min, and then held at 310°C for more

99 than 30 min. Helium was used as the carrier gas, with a flow rate of 30 cm/s. Selected samples were
 100 performed using GC-MS for compound identification. The GC column and oven temperature program was
 101 the same as GC-FID. The mass spectrometer was run in full scan mode (m/z 50–650). Electron ionization
 102 (EI) spectra were obtained at 70 eV. Alkenones were identified using an external standard by GC retention
 103 times by analogy with a synthetic standard (provided by M. Yamamoto, Hokkaido University, Japan) and
 104 characteristic mass fragments. *N*-alkanes were identified by comparing mass spectra and retention times
 105 with those of the standards and published data.

106 The carbon preference index (CPI; Bray and Evans 1961) of C_{26} - C_{34} homologues and the average
 107 chain length (ACL) of odd C_{27} - C_{35} homologues (Duan and He 2011) used in this study were as follows:
 108

$$109 \quad CPI = \left(\frac{C_{27} + C_{29} + C_{31} + C_{33}}{C_{26} + C_{28} + C_{30} + C_{32}} + \frac{C_{27} + C_{29} + C_{31} + C_{33}}{C_{28} + C_{30} + C_{32} + C_{34}} \right) / 2 \quad (1)$$

$$111 \quad ACL = \frac{27 \times C_{27} + 29 \times C_{29} + 31 \times C_{31} + 33 \times C_{33} + 35 \times C_{35}}{C_{27} + C_{29} + C_{31} + C_{33} + C_{35}} \quad (2)$$

112
 113 The $[C_{26}$ - $C_{35}]$ are concentration of odd and even *n*-alkane. The $U_{37}^k = ([C_{37:2}$ - $C_{37:4}] / [C_{37:2} + C_{37:3} +$
 114 $C_{37:4}])$ index has been proposed to quantify the degree of alkenone unsaturation (Brassell et al. 1986),
 115 which is a function of SST. Because $C_{37:4}$ is often absent in open ocean sediments when SSTs are higher
 116 than 12°C (Prah and Wakeham 1987), the index was simplified to $U_{37}^{k'} = ([C_{37:2}] / [C_{37:2} + C_{37:3}])$. We
 117 converted the index values to SST using the widely used *Emiliana huxleyi* culture-based calibration
 118 proposed by Prah et al. (1988), $U_{37}^k = 0.04 T - 0.104$ ($r^2 = 0.98$) and $U_{37}^{k'} = 0.034 T + 0.039$ ($r^2 = 0.99$),
 119 and the simplified $U_{37}^{k'}$ calibration based on global core top compilations (Conte et al. 2006).
 120

121 2.5 Carbon isotope analysis

122
 123 The carbon isotope ratio of *n*-alkanes was performed using a gas chromatograph with a DB-5MS
 124 column (60 m × 320 μm × 250 μm) interfaced to a Thermofisher MAT-253 isotope-ratio mass
 125 spectrometer via a combustion interface (960°C) consisting of an alumina reactor containing nickel and
 126 platinum wires. Helium was used as the carrier gas with a flow rate of 1.2ml/min using splitless injecting.
 127 The oven temperature was programmed from 80 to 100°C at 10°C/min, 100 to 220°C at 4°C/min, 220 to
 128 280°C at 2°C/min, and then held at 280°C for 15 mins. All samples are injected one time for carbon
 129 isotope analysis. The analytical error was calculated based on the reproduced analytical results of an

external standard, injected once after every sixth sample injection, and had an analytical error of 0.7‰ (1σ). The pre-calibrated isotopic composition of CO₂ was used as a standard. All δ¹³C values were expressed versus VPDB.

Based on the isotopic values of *n*-alkanes, we can quantify the percentage source of long-chain *n*-alkanes from C₃/C₄ plants using a binary isotope mass balance model (Thomas et al. 2014):

$$\delta^{13}C_s = f \times \delta^{13}C_{C_3} + (1-f) \times \delta^{13}C_{C_4} \quad (3)$$

where δ¹³C_s are the long-chain *n*-alkanes from sediments, δ¹³C_{C₃} and δ¹³C_{C₄} are the carbon isotopic values of long-chain *n*-alkanes from C₃ and C₄ terrestrial higher vascular plants, respectively, and *f* is the proportion of long-chain *n*-alkanes from C₃ plants. We set the carbon isotopic values of long-chain *n*-alkanes for C₃ and C₄ plants to be -36‰ and -22‰, respectively (Chikaraishi and Naraoka 2007; Vogts et al. 2009). C₃₁ *n*-alkane abundance is relatively higher than C₂₉ and C₃₃ *n*-alkanes; thus, we use the carbon isotopic values of C₃₁ *n*-alkane to calculate the percentage source of long-chain *n*-alkanes from C₃/C₄ plants.

3. Results

3.1 Concentration and distribution of long-chain *n*-alkanes

In the 12 pilot samples from the core R23, we found a significant change in the concentrations of total long-chain *n*-alkanes (C₂₃-C₃₅) in the sediment profile, ranging from 295-787 ng/g (Table 1, Table S1, Fig. 2). The distribution pattern of long-chain *n*-alkanes (C₂₃-C₃₅) in each sediment sample was similar, with bimodal distributions peaking at C₂₃-C₂₅ and C₂₇ or C₃₁ (Fig. 3). However, there was no apparent predominant odd-over-even carbon preference, and CPI₂₇₋₃₃ varied from 1.1-2.5, with an average of 1.7 (Fig. 2). The distribution patterns of long-chain *n*-alkanes were divided into two types. One is mid-chain *n*-alkanes (C₂₃-C₂₇), with no predominant odd-over-even carbon preference (CPI ~1), and the other is long-chain *n*-alkanes (C₂₉-C₃₅) with dominant odd-over-even carbon preference. The ACL values of long-chain *n*-alkanes (C₂₇-C₃₅) were in the range of 29.3-30.7. The ACL values are strongly correlated with CPI (Fig. 4).

3.2 Concentration and distribution of alkenones

162

163 $C_{37:4}$, $C_{37:3}$, and $C_{37:2}$ alkenones were all detected in the 12 pilot samples, with total concentrations
164 ranging from 12.6-104.2 ng/g sediment dry wt (Table 2). The distribution pattern of three unsaturated
165 alkenones revealed significant differences among the subsamples, and the relative abundance of $C_{37:4}$, $C_{37:3}$,
166 and $C_{37:2}$ varied from 11-37%, 27-87%, and 3-48%, respectively. The tri-unsaturated alkenone ($C_{37:3}$) was
167 the most abundant in the sediments. Interestingly, a high abundance of tetra-unsaturated alkenone was
168 found in the sediment samples. The SST estimates we inferred from the U_{37}^k and $U_{37}^{k'}$ indexes are
169 between -1.7 to 8.4°C and -0.4 to 17.9°C, respectively.

170

171 3.3 The carbon isotopes of individual *n*-alkanes

172

173 Our *n*-alkane-specified carbon isotope analysis of the 12 pilot samples shows a significant change.
174 Therefore, based on the chain length of the *n*-alkanes, we divided *n*-alkanes into two endmembers (Table
175 1). One is mid-chain *n*-alkanes, which had $\delta^{13}C$ values ranging from -31.5 to -25.4‰ and -32.3 to -26.7‰,
176 with an average of -28.6‰ and -29.4‰ for C_{23} and C_{25} , respectively. The other is long-chain *n*-alkanes
177 (C_{27} , C_{29} , and C_{31}), with $\delta^{13}C$ values from -30.1 to -26.3‰ (C_{27} , averaging -28.0‰), -30.4 to -25.0‰ (C_{29} ,
178 averaging -27.5‰) and -29.4 to -24.8‰ (C_{31} , averaging -26.9‰). The average $\delta^{13}C$ values of long-chain
179 *n*-alkanes (C_{27} , C_{29} , and C_{31}) were higher than mid-chain *n*-alkanes (C_{23} and C_{25}). C_{26} and C_{28} *n*-alkanes
180 had the lowest $\delta^{13}C$ values averaging \sim -34‰. The percentage source of long-chain *n*-alkanes from C_3/C_4
181 plants using C_{31} $\delta^{13}C$ values varied from 47-80% for C_4 plants (Table 1).

182

183 4. Discussion

184

185 4.1 Source of mid-chain *n*-alkanes

186

187 Our pilot study indicates that the mid-chain *n*-alkanes (C_{23} - C_{25}) are abundant with no predominant
188 odd-over-even carbon preference in the sediment profile (CPI \sim 1; Fig. 3), and the contamination of
189 petroleum may cause this during coring and sampling. However, our sampling procedures by the crew of
190 the R/V Xuelong in the 31st CHINARE have been devised to prevent any possible contamination by
191 petroleum, and no signs of petroleum contamination have been observed while treating sediment samples
192 in the laboratory. All lab-ware was baked at 450°C in a furnace before using to prevent contamination
193 during the analysis of the samples. Blank experiments were also analyzed, and negligible contamination
194 was found. Furthermore, the average $\delta^{13}C$ values of *n*-alkanes with different chain lengths are different

(Table 1, Fig. 5). For example, the average $\delta^{13}\text{C}$ values of mid-chain *n*-alkanes ($\text{C}_{23}\text{-C}_{25}$) were similar to the *n*-alkanes from marine phytoplankton (Ashley et al. 2020). Therefore, it is very unlikely that these *n*-alkanes were due to petroleum contamination during coring and sampling. The abundant mid-chain *n*-alkanes ($\text{C}_{23}\text{-C}_{25}$) with no predominant odd-over-even carbon preference were natural characteristics in the sediment samples of core R23.

Several studies have shown that ocean phytoplankton can produce mid-chain *n*-alkanes and *n*-alkanoic acids (e.g., Volkman et al. 1998). *N*-alkanoic acids are biosynthesized in the acetogenic pathway, and then they are converted to *n*-alkanes by enzymatic decarboxylation; thus, they have similar distributions (Diefendorf and Freimuth 2017). Mid-chain *n*-alkanoic acids ($\text{C}_{22}\text{-C}_{24}$) can be produced by marine plants, such as marine microalgae, diatoms, and seaweed (Naraoka and Ishiwatari 2000). Thus, phytoplankton may be a significant source for these mid-chain *n*-alkanes with no predominant odd-over-even carbon preference ($\text{CPI} \sim 1$). A previous study has reported that the average $\delta^{13}\text{C}$ values of *n*-alkanoic acids produced by marine phytoplankton were about -28‰ (Ashley et al. 2020). In our pilot analysis of the 12 samples, the average $\delta^{13}\text{C}$ values of *n*-alkanes with different chain lengths vary greatly. The $\delta^{13}\text{C}$ values of mid-chain *n*-alkanes ($\text{C}_{23}\text{-C}_{25}$; $\sim -29\text{‰}$) are in the range of *n*-alkanes from marine organisms, and soil samples ($\sim -28\text{‰}$) in the McMurdo Dry Valleys (Hayes et al. 1990; Ishiwatari et al. 1994; Matsumoto et al. 2010), but are lower than lake sediments ($\sim -15\text{‰}$) with shallow water depth from East Antarctica (Chen et al. 2019). Thus, the terrestrial organic matter from ice-free areas of Antarctica transported by ice-rafted debris (IRD) and aeolian may also contribute to mid-chain *n*-alkanes (Chewings et al. 2014). Still, the source from shallow lake sediments at higher latitudes was considered negligible. The $\delta^{13}\text{C}$ values of C_{26} and C_{28} are lower than other long-chain *n*-alkanes (Fig. 5), suggesting they may have other sources. Moreover, the $\delta^{13}\text{C}$ values of C_{26} and C_{28} in our study samples are also obviously depleted relative to marine organisms and soil samples from Antarctica. The C_{26} and C_{28} may likely originate from chemoautotrophic bacteria because they have relatively low $\delta^{13}\text{C}$ values and have no odd-over-even predominance (Hayes et al. 1990; Collister et al. 1994). Thus, from the above discussion, we believe that mid-chain *n*-alkanes (C_{23} to C_{25}) have mixing sources, including marine (non-diatom pelagic phytoplankton and marine microalgae) and terrestrial organic matter, but C_{26} and C_{28} *n*-alkanes might be originated mainly from chemoautotrophic bacteria.

4.2 Sources of long-chain *n*-alkanes

There are three major sources for long-chain *n*-alkanes ($\text{C}_{27}\text{-C}_{35}$) in the South Pacific sector of the Southern Ocean sediments, including long-range transport of dust from lower latitudes, ocean plankton,

228 and sediments eroded from Antarctica. Previous studies have shown that short- and mid-chain *n*-alkanes
229 are predominant in Pleistocene age ocean sediments, modern water column suspended particulate matter in
230 the Ross Sea and Antarctic margin, while long-chain *n*-alkanes have a minor contribution (Harada et al.
231 1995; Hayakawa et al. 1996; Cincinelli et al. 2008). Moreover, the $\delta^{13}\text{C}$ values of *n*-alkanes ranged from
232 -28.5 to -26.2‰, suggesting that their major source was possibly derived from marine organisms (Harada
233 et al. 1995). In the Ross Sea, abundant long-chain *n*-alkanes with low CPI values in ocean sediments have
234 suggested that the organic matter was mainly originated from altered or recycled material mixed with
235 modern marine input (Kvenvolden et al. 1987; Venkatesan 1988; Duncan et al. 2019). Long-range
236 transport of terrestrial organic matter and higher plant leaf waxes is also an important source for
237 long-chain *n*-alkanes in the Pacific sector of the Southern Ocean (Bendle et al. 2007; Martinez-Garcia et al.
238 2009, 2011; Lamy et al. 2014; Jaeschke et al. 2017). For example, Bendle et al. (2007) studied organic
239 geochemical characteristics in Southern Ocean aerosol samples. The results showed that the abundant
240 long-chain *n*-alkanes with relatively low $\delta^{13}\text{C}$ values (-37 to -30.8‰) represented a regional background of
241 well-mixed higher vascular plants through long-range transportation.

242 The core R23 is near the Antarctic continent, and so the organic matter from Antarctica may be a
243 potential source of long-chain *n*-alkanes at our site. However, there are no vascular plants in the Antarctic,
244 except for limited terrestrial vegetation (moss and lichen) in relatively low latitudes of the Antarctic
245 Peninsula. Dust contribution from terrestrial material through aeolian transportation is negligible due to the
246 lack of exposed, mature soils in the McMurdo Dry Valleys and Victoria Land (Nylen et al. 2004; Lewis et
247 al. 2008, 2016), as well as the long-distance of the core site from the coast. Moreover, Mastumoto et al.
248 (2010) have reported that the chain length of *n*-alkanes ranging from C_{15} - C_{37} was found in McMurdo Dry
249 Valley soil, with the majority as C_{23} , C_{25} , and C_{27} *n*-alkanes, but with extremely low abundance of C_{29} and
250 C_{31} *n*-alkanes. Recently, Chen et al. (2019) reported that abundant long-chain *n*-alkanes with highly
251 enriched carbon isotopic ratios (\sim -25 to -12‰) in shallow lake sediments from East Antarctica (no vascular
252 plants are present in the surrounding landmass) were predominantly derived from heterotrophic microbes.
253 However, the average $\delta^{13}\text{C}$ values of long-chain *n*-alkanes (C_{27} , C_{29} , and C_{31}) varying from \sim -28 to -27‰
254 in the R23 sediments are lower than these in the lacustrine sediments from East Antarctica. Therefore, the
255 sources of long-chain *n*-alkanes (C_{27} - C_{35}) from ice-free soils and shallow lacustrine sediments in East
256 Antarctica via dust transport and ocean phytoplankton is negligible.

257 The ACL of long-chain *n*-alkanes refers to the average number of carbon atoms/molecule and can
258 indicate their source (Poynter and Eglinton 1990). The ACL values of long-chain *n*-alkanes (C_{27} - C_{35})
259 ranged from 29.3-30.7 in the sediment samples, similar to Southern Ocean ACL values with a range of
260 29.1-30.6 in the surface sediments, both indicating the significant contribution of higher plants (Jaeschke

261 et al. 2017). A significant linear relationship was observed between ACL and CPI ($n = 12$, $r^2 = 0.54$, $p <$
262 0.01 ; Fig. 4). Generally, relatively high CPI values ($CPI > 3$) indicate long-chain *n*-alkanes from higher
263 vascular plants, while low CPI values ($CPI \sim 1$) may imply post-depositional degradation and mature
264 organic matter inputs (Eglinton and Eglinton 2008; Duncan et al. 2019). According to leaf litter
265 degradation experiments, the odd-over-even predominance of *n*-alkanes was observed to decline. The
266 long-chain *n*-alkanes ratios (e.g., C_{31}/C_{29}) were tended to ~ 1 (Zech et al. 2011). Based on this result, it is
267 reasonable to infer that *n*-alkanes in the dust might have experienced a certain degree of degradation
268 during long-range transportation and post-deposition, which could result in low CPI values. Furthermore,
269 relatively low CPI values of 1.1 to 2.5 present in the R23 sediment core may also be considered to
270 microbial degradation under very low sedimentation rates < 2 cm/ka (Tiedemann 2012; Jaeschke et al.
271 2017; Duncan et al. 2019). Previous studies have shown that the average sedimentation rates were as low
272 as 1.18 cm/ka in Prydz Bay (Wu et al. 2015) and 1.00 cm/ka in ODP 1167 (Theissen et al. 2003). Low
273 CPIs and low sedimentation rates in the DSDP 274 sediment core from the northwest Ross Sea suggest
274 that long-chain *n*-alkanes have been extensively degraded by bacterial activity in the seabed surface layers
275 (Duncan et al. 2019). Under the condition of degradation, the $\delta^{13}C$ values of long-chain *n*-alkanes have no
276 obvious difference (Huang et al. 1997; Li et al. 2017); thus, it could be useful to trace the sources of
277 organic matter and reconstruct the paleoecological changes. The high abundance of long-chain even
278 *n*-alkanes (C_{26} and C_{28}) with lower $\delta^{13}C$ values in the R23 sediment core indicates microbial
279 (chemoautotrophic) activity in this region. Altered or recycled organic matter from Antarctica that has
280 been eroded by glaciers and transported by IRD is important in the study region (Chewings et al. 2014;
281 Duncan et al. 2019). Therefore, we suggest that the long-chain *n*-alkanes (C_{29} - C_{35}) primarily originated
282 from terrestrial higher plant waxes via long-range transport of dust from lower latitude continental regions
283 (e.g., Australia and New Zealand), and altered or recycled organic matter from Antarctica may be another
284 secondary source.

285 Our results are consistent with previous studies in the Southern Ocean. Long-chain *n*-alkanes were
286 reported to originate mainly from long-range transport of dust from Australia and New Zealand by
287 prevailing westerlies (Martinez-Garcia et al. 2011; Lamy et al. 2014). For example, relatively enriched
288 carbon isotopic ratios of C_{31} *n*-alkane in the surface sediments from the Australian sector of the Southern
289 Ocean suggest significant contributions of C_4 higher vascular plant waxes (Ohkouchi et al. 2000). More
290 recently, Jaeschke et al. (2017) have reported that the CPI values of long-chain *n*-alkanes ranged from
291 1.1-10 in the Pacific sector of the Southern Ocean, indicating the contribution of higher plant leaf waxes.
292 Because the location of surface sediments in our study site is far from the potential source regions of land
293 continents (New Zealand and Australia), it is reasonable to believe that the long-chain *n*-alkanes in the R23

294 sediment core are primarily derived from terrestrial higher plant leaf wax through long-range eolian
295 transportation.

297 4.3 Estimation of C₃/C₄ plant fraction

298
299 As discussed above, the long-chain *n*-alkanes (C₂₇, C₂₉, and C₃₁) in R23 sediments are primarily
300 derived from higher plant leaf waxes by long-range transport of dust. Interestingly, the δ¹³C values of
301 long-chain *n*-alkanes were 5-10‰ higher than those in C₃ plants. This difference indicates that
302 considerable amounts of *n*-alkanes are derived from C₄ plant waxes, which have significantly higher
303 carbon isotopic values. The relative contributions of long-chain *n*-alkanes (C₂₇, C₂₉, and C₃₁) from C₃ and
304 C₄ plants are significantly different in the sediment samples. For the carbon isotopic values of C₃₁
305 *n*-alkanes, 80% originated from C₄ plants in the 398cm section; however, only 47% originated from C₄
306 plants in the 762 cm section (Table 1). Ohkouchi et al. (2000) reported that the relative contributions of C₃₁
307 *n*-alkanes from C₃ and C₄ plants are about 60% and 40% in the surface sediments from the Australian
308 sector of the Southern Ocean respectively (Ohkouchi et al. 2000). Previous studies have demonstrated that
309 the primary drivers for the distributions of C₃/C₄ plants are climatic and atmospheric *p*CO₂ etc. (Huang et
310 al. 2001; Edwards et al. 2010). Compared with C₃ plants, C₄ grasses usually favor relatively lower *p*CO₂
311 and arid conditions due to their greater water use efficiency and carbon concentrating mechanism
312 (Edwards et al. 2010). Therefore, the different contributions of C₃/C₄ plants may be related to climate
313 change (e.g., temperature and precipitation) in the source regions (Huang et al. 2001). Based on the above
314 discussion, it is reasonable to infer that the source of the long-chain *n*-alkanes was mainly derived from
315 long-range transport of dust from New Zealand and Australia (Neff and Bertler 2015). Therefore, these
316 results indicate that the δ¹³C values of long-chain *n*-alkanes could be used to reconstruct the past changes
317 of C₃/C₄ plants in the source area and then investigate climatic variations.

319 4.4 Assessing U₃₇^k and U₃₇^{k'}-derived SST records

320
321 C_{37:4} alkenone was found in the R23 sediments with relative abundance ranging from 11-37%. This is
322 similar to a previous study in the higher latitude of the Pacific sector of the Southern Ocean (Sikes et al.
323 1997) but significantly higher than the sedimentary abundance from the lower latitudes of the Southern
324 Ocean (Jaeschke et al. 2017). Previous studies have shown that C_{37:4} is often absent in open ocean sediments
325 where SSTs are higher than 12°C (Prah et al. 1987). The modern annual SST in our study site is about 0°C;
326 thus, the high abundance of C_{37:4} alkenone may be related to the extremely low temperature. Numerous

327 studies have demonstrated that a high abundance of C_{37:4} in surface sediments is related to low-temperature
328 and low-salinity surface water masses in the Arctic (Sicre et al. 2002; Bendle et al. 2005; Harada et al. 2006,
329 2012). Analysis of 106 surface water and sediment samples from the Atlantic, Pacific, and the Southern
330 Ocean indicated that the relative abundance of C_{37:4} methyl alkenone had no apparent relationship with SST
331 and salinity. Still, it might respond to some other environmental factors, including growth rate, light, or
332 nutrients (Sikes and Sicre 2002). For example, %C_{37:4} showed a negative linear correlation with sea surface
333 salinity (SSS), nutrients and late summer SST in the suspended particles and sediment profiles from the
334 Bering Sea (Harada et al., 2012). However, SST and SSS showed a strong negative linear relationship in the
335 north Atlantic and the Bering Sea because of sea ice melting during the summer season, suggesting that the
336 relationship of %C_{37:4} and salinity may be the artifact the covariance with temperature (Sikes and Sicre
337 2002). Moreover, up until now, most samples were from the Atlantic and Pacific Oceans, and there were few
338 studies on the distributional characteristics of alkenones in the high latitudes of the Southern Ocean.

339 To determine whether SST affects the relative abundance of C_{37:4} methyl alkenone, we calculated the
340 sea surface temperature based on the U₃₇^k and U₃₇^{k'} index using the formula reported by Prahl et al. (1988)
341 and Conte et al. (2006), respectively (Table 2). Our results show that SST data between U₃₇^k- and U₃₇^{k'}-SST
342 was, as we expected, obviously different (Fig. 6). When the relative abundance of tetra-unsaturated alkenone
343 was higher, we found U₃₇^{k'}-SST was warmer than U₃₇^k-SST in 166, 243, 323, 550, 626, 762 and 818 cm
344 sediment sections, and the difference between U₃₇^{k'} and U₃₇^k-SST is in the range of 4.8-10.9°C. However,
345 the SST difference calculated by these two indexes is relatively small in the sediment sections of the lower
346 abundance of C_{37:4} alkenone. Based on the average summer SST from the World Ocean Atlas (WOA09) data
347 set (Locarnini et al. 2010), the modern sea surface temperature in our study site was about 0-1°C. For the
348 historical period, the highest subsurface temperature is about 4-5°C during the Holocene at similar latitudes,
349 including the eastern Antarctic continental margin (Kim et al. 2012) and western Antarctic Peninsula
350 (Etourneau et al. 2013). According to modern observation and SST reconstruction during the late
351 Pleistocene, we suggest that the highest SST in our study site should be lower than 5°C in the warmer
352 periods, which was much lower than U₃₇^{k'}-SST. Therefore, all these results indicate higher %C_{37:4} is most
353 likely controlled by extremely low SST in the R23 sediments and the U₃₇^k index is more feasible than U₃₇^{k'}
354 in the relatively higher latitudes of the Southern Ocean.

355 Ho et al. (2012) also found the U₃₇^{k'}-SST records were significantly warmer in glacial periods, and that
356 the U₃₇^k index is a more suitable SST proxy in the sub-Antarctic and higher latitude Pacific (Ho et al. 2012;
357 Haddam et al. 2018). Other studies have shown a significant relationship between the relative abundance of
358 C_{37:4} and temperature (Prahl et al. 1988). Moreover, several other studies indicate %C_{37:4} is closely related to
359 cold water mass expansion (Bard et al. 2000; Martínez-García et al. 2010). Although the influencing factors

360 on the relative abundance of C_{37:4} alkenone are complex, a statistically significant relationship between U₃₇^k
361 index and SST has been found in the surface sediments from high latitudes of the North Atlantic Ocean
362 (Rosell-Melé et al. 1995). This result further validates the general applicability of the U₃₇^k as a reliable
363 climatic proxy for SST reconstructions in the relatively cold climate regions (Rosell-Melé et al. 1994, 1995).
364 The latitude was relatively high at our study site, and the modern annual summer SST was lower than 1°C.
365 The marine algae may synthesize more C_{37:4} alkenones to adapt to the extremely cold conditions. Notably,
366 there are few U₃₇^k-SST records in the Southern Ocean at latitudes higher than 60°S. Therefore, our study
367 indicates that the usage of the U₃₇^k index is feasible for reconstructing past SST in the Southern Ocean, but
368 more studies on surface water and sediment samples in high latitudes are required to confirm the relationship
369 between C_{37:4} alkenones and sea surface temperature.

371 5. Conclusions

372
373 We have presented pilot results of the relative distribution and individual δ¹³C values of long-chain
374 *n*-alkanes and the organic geochemical characterization of alkenones in 12 samples selected from a
375 sediment core collected from the Pacific sector of the Southern Ocean. Our results suggest that the
376 abundant long-chain *n*-alkanes (C₂₇-C₃₅) with a significant odd-over-even carbon preference might have
377 originated from terrestrial higher plant waxes, possibly via long-range transport of dust from Australia and
378 New Zealand. The mid-chain *n*-alkanes (C₂₃-C₂₅) preserved in the sediments have low odd-over-even
379 carbon preference, perhaps indicating mixing of marine (non-diatom pelagic phytoplankton and marine
380 microalgae) and terrestrial sources. The C₂₆ and C₂₈ *n*-alkanes with relatively lower δ¹³C values indicate an
381 origin from marine chemoautotrophic bacteria. The δ¹³C values of long-chain *n*-alkanes (C₂₇-C₃₁) range
382 between -30.8 to -24.8‰ in the sediments, approximately 5-10‰ higher than in terrestrial C₃ higher plants.
383 Furthermore, the relative abundance of tetra-unsaturated alkenone in the sediments varies from 11 to 37%,
384 higher than those previously reported in the lower latitudes of the South Pacific Ocean. We conclude that
385 tetra-unsaturated alkenones are sensitive markers of low SSTs, suggesting the feasibility of using U₃₇^k in
386 further SST reconstructions in the Pacific sector of the Southern Ocean.

393 **Acknowledgments**

394 This work was jointly supported by the National Natural Science Foundation of China (grant nos. 41776188,
395 41576183, 41476172 and 41772366) and MOST funding (MOST 106-2116-M-019-007). We are grateful to
396 the crew of the R/V Xuelong for their assistance with sample collection in the 31st CHINARE, and thanks to
397 Chinese Projects for Investigations and Assessments of the Arctic and Antarctic (CHINARE2012-2020 for
398 01-04, 02-01 and 03-04). We also acknowledge S. Emslie for editing and Tiegang Li for providing samples.

399

400 **Author's contributions**

401 Min-Te Chen, Xiaodong Liu, and Xin Chen proposed the topic, conceived and designed the study, and they
402 wrote the draft of this paper. Xin Chen and Da-Cheng Lin conducted the experiments. All the co-authors
403 contributed to the discussion and edited and commented on the paper. All authors read and approved the
404 final manuscript.

405

406 **Funding**

407 This study was supported by grant numbers 41776188, 41576183, 41476172, and 41772366 from the
408 National Natural Science Foundation of China and the Joint Projects of MOST (Ministry of Science and
409 Technology) to MTC. This work is also partly supported by the Chinese Projects for Investigations and
410 Assessments of the Arctic and Antarctic (CHINARE2012-2020 for 01-04, 02-01, and 03-04) to LQC.

411

412 **Availability of data and materials**

413 The datasets in the current study are available from the corresponding author on reasonable request.

414

415 **Competing interests**

416 The authors declare that they have no competing interests.

417

418 **References:**

- 419 Ashley K, Bendle J, Crosta X, Etourneau J, Campagne P, Gilchrist H, Ibraheem U, Greene S, Schmidt S,
420 Eley Y, Massé G (2020) Fatty acid carbon isotopes: a new indicator of marine Antarctic
421 paleoproductivity? *Biogeosciences Discuss.* <https://doi.org/10.5194/bg-2020-124>
- 422 Bard E, Rostek F, Turon JL, Gendreau S (2000) Hydrological impact of Heinrich events in the subtropical
423 northeast Atlantic. *Science* 289:1321-1324
- 424 Bendle J, Kawamura K, Yamazaki K, Niwai T (2007) Latitudinal distribution of terrestrial lipid
425 biomarkers and n-alkane compound-specific stable carbon isotope ratios in the atmosphere over the
426 western Pacific and Southern Ocean. *Geochim Cosmochim Acta* 71:5934-5955,
- 427 Bendle J, Rosell - Melé A, Ziveri P (2005) Variability of unusual distributions of alkenones in the surface
428 waters of the Nordic seas. *Paleoceanography* 20:PA2001. <https://doi.org/10.1029/2004PA001025>
- 429 Brassell SC, Eglinton G, Marlowe IT, Pfaumann U, Sarnthein M (1986) Molecular stratigraphy: a new tool
430 for climatic assessment. *Nature* 320:129-133
- 431 Bray EE, Evans ED (1961) Distribution of n-paraffins as a clue to recognition of source beds. *Geochim*
432 *Cosmochim Acta* 22:2-15
- 433 Bubba MD, Cincinelli A, Checchini L, Lepri L, Desideri P (2004) Horizontal and vertical distributions of
434 Biogenic and Anthropogenic Organic compounds in the Ross Sea (Antarctica). *Int J Environ Anal*
435 *Chem* 8:441-456
- 436 Chen X, Liu X, Wei Y, Huang, Y (2019) Production of long chain n-alkyl lipids by heterotrophic microbes:
437 new evidence from Antarctic lakes. *Org Geochem* 138:103909.
438 <https://doi.org/10.1016/j.orggeochem.2019.103909>
- 439 Chewings JM, Atkins CB, Dunbar GB, Golledge NR (2014) Aeolian sediment transport and deposition in
440 a modern high - latitude glacial marine environment. *Sedimentology* 61:1535-1557
- 441 Chikaraishi Y, Naraoka H (2007) $\delta^{13}\text{C}$ and δD relationships among three n-alkyl compound classes
442 (n-alkanoic acid, n-alkane and n-alkanol) of terrestrial higher plants. *Org Geochem* 38:198-215
- 443 Cincinelli A, Martellini T, Bittoni L, Russo A, Gambaro A, Lepri L (2008) Natural and anthropogenic
444 hydrocarbons in the water column of the Ross Sea (Antarctica). *Journal of Marine*
445 *Systems* 73:208-220
- 446 Collister JW, Lichtfouse E, Hieshima G, Hayes JM (1994) Partial resolution of sources of n-alkanes in the
447 saline portion of the Parachute Creek Member, Green River Formation (Piceance Creek Basin,
448 Colorado). *Org Geochem* 21:645-659
- 449 Conte MH, Sicre MA, Rühlemann C, Weber JC, Shultz-Bull D, Blanz T (2006) Global temperature
450 calibration of the alkenone unsaturation index ($U^{K'_{37}}$) in surface waters and comparison with surface

451 sediments. *Geochem Geophys Geosyst* 7:Q02005. <https://doi.org/10.1029/2005GC001054>

452 Diefendorf AF, Freimuth EJ (2017) Extracting the most from terrestrial plant -derived n-alkyl lipids and
453 their carbon isotopes from the sedimentary record: A review. *Org Geochem* 103:1-21

454 Duan Y, He J (2011) Distribution and isotopic composition of n-alkanes from grass, reed and tree leaves
455 along a latitudinal gradient in China. *Geochem J* 45:199-207

456 Duncan B, McKay R, Bendle J, Naish T, Inglis GN, Moossen H, Levy R, Ventura GT, Lewis A,
457 Chamberlain B, Walker C (2019) Lipid biomarker distributions in Oligocene and Miocene sediments
458 from the Ross Sea region, Antarctica: implications for use of biomarker proxies in
459 glacially-influenced settings. *Palaeogeogr Palaeoclimatol Palaeoecol* 516:71-89

460 Edwards EJ, Osborne CP, Stromberg CA, Smith SA (2010) The Origins of C₄ Grasslands: Integrating
461 Evolutionary and Ecosystem Science. *Science* 328: 587-591

462 Eglinton TI, Eglinton G (2008) Molecular proxies for paleoclimatology. *Earth Planet Sci Lett* 275:1-16

463 Etourneau J, Collins LG, Willmott V, Kim JH, Barbara L, Leventer A, Schouten S, Sinninghe Damste JS,
464 Bianchini A, Klien V, Crosta X, Massé G (2013) Holocene climate variations in the western Antarctic
465 Peninsula: evidence for sea ice extent predominantly controlled by changes in insolation and ENSO
466 variability. *Climate of the Past* 9:1431-1446

467 Fischer H, Schmitt J, Lüthi D, Stocker TF, Tschumi T, Parekh P, Joos F, Köhler P, Völker C, Gersonde R,
468 Barbante C, Le Floch M, Raynaud D, Wolff EW (2010) The role of Southern Ocean processes in
469 orbital and millennial CO₂ variations—A synthesis. *Quat Sci Rev* 29:193-205

470 Haddam NA, Siani G, Michel E, Kaiser J, Lamy F, Duchamp-Alphonse S, Hefter J, Braconnot P, Dewilde F,
471 Isgüder G, Tisnerat-Laborde N, Thil F, Durand N, Kissel C (2018) Changes in latitudinal sea surface
472 temperature gradients along the Southern Chilean margin since the last glacial. *Quat Sci*
473 *Rev* 194:62-76

474 Harada N, Handa N, Fukuchi M, Ishiwatari R (1995) Source of hydrocarbons in marine sediments in
475 Lützow-Holm Bay, Antarctica. *Org Geochem* 23:229-237

476 Harada N, Sato M, Oguri K, Hagino K, Okazaki Y, Katsuki K, Tsuji Y, Shin KH, Tadai O, Saitoh SI, Narita
477 H, Konno S, Jordan RW, Shiraiwa Y, Grebmeier J (2012) Enhancement of coccolithophorid blooms in
478 the bering sea by recent environmental changes. *Global Biogeochem. Cycles* 26, GB2036,
479 [doi:10.1029/2011GB004177](https://doi.org/10.1029/2011GB004177)

480 Harada N, Sato M, Shiraishi A, Honda MC (2006) Characteristics of alkenone distributions in suspended
481 and sinking particles in the northwestern North Pacific. *Geochim Cosmochim Acta* 70:2045-2062

482 Hayakawa K, Handa N, Ikuta N, Fukuchi M (1996) Downward fluxes of fatty acids and hydrocarbons
483 during a phytoplankton bloom in the austral summer in Breid Bay, Antarctica. *Org*

484 Geochem 24:511-521

485 Hayes JM, Freeman KH, Popp BN, Hoham CH (1990) Compound-specific isotopic analyses: a novel tool
486 for reconstruction of ancient biogeochemical processes. *Org Geochem* 16:1115-1128

487 Ho SL, Mollenhauer G, Lamy F, Martinez-Garcia A, Mohtadi M, Gersonde R, Hebbeln D, Nunez-Ricardo
488 S, Rosell-Mele A, Tiedemann R (2012) Sea surface temperature variability in the Pacific sector of the
489 Southern Ocean over the past 700 kyr. *Paleoceanography* 27:PA4202.
490 <https://doi.org/10.1029/2012PA002317>

491 Holtvoeth J, Whiteside JH, Engels S, Freitas FS, Grice K, Greenwood P, Johnson S, Kendall I, Lengger
492 SK, Lücke A, Mayr C, Naafs BDA, Rohrsen M, Sepúlveda J (2019) The paleolimnologist's guide to
493 compound-specific stable isotope analysis – An introduction to principles and applications of CSIA
494 for Quaternary lake sediments. *Quat Sci Rev* 207:101–133

495 Huang Y, Eglinton G, Ineson P, Latter PM, Bol R, Harkness DD (1997) Absence of carbon isotope
496 fractionation of individual n-alkanes in a 23-year field decomposition experiment with *Calluna*
497 *vulgaris*. *Org Geochem* 26:497-501

498 Huang Y, Street-Perrott FA, Metcalfe SE, Brenner M, Moreland M, Freeman K (2001) Climate change as
499 the dominant control on glacial-interglacial variations in C₃ and C₄ plant
500 abundance. *Science* 293:1647-1651

501 Ishiwatari R, Uzaki M, Yamada K (1994) Carbon isotope composition of individual n-alkanes in recent
502 sediments. *Org Geochem* 21:801-808

503 Jaeschke A, Wengler M, Hefter J, Ronge TA, Geibert W Mollenhauer G, Lamy F (2017) A biomarker
504 perspective on dust, productivity, and sea surface temperature in the Pacific sector of the Southern
505 Ocean. *Geochim Cosmochim Acta* 204:120-139

506 Kim JH, Crosta X, Willmott V, Renssen H, Bonnin J, Helmke P, Schouten S, Sinninghe Damste JS (2012)
507 Holocene subsurface temperature variability in the eastern Antarctic continental margin. *Geophys Res*
508 *Lett* 39:L06705. <https://doi.org/10.1029/2012GL051157>

509 Kohfeld KE, Graham RM, De Boer AM, Sime LC, Wolff EW, Le Quéré C, Bopp L (2013) Southern
510 Hemisphere westerly wind changes during the Last Glacial Maximum: paleo-data synthesis. *Quat Sci*
511 *Rev* 68:76-95

512 Kvenvolden KA, Rapp JB, Golan-Bac M, Hostettler FD (1987) Multiple sources of alkanes in Quaternary
513 oceanic sediment of Antarctica. *Org Geochem* 11:291-302

514 Lamy F, Gersonde R, Winckler G, Esper O, Jaeschke A, Kuhn G, Ullermann J, Martínez-Garcia A,
515 Lambert F, Kilian R (2014) Increased dust deposition in the Pacific Southern Ocean during glacial
516 periods. *Science* 343:403-407

517 Lamy F, Kilian R, Arz HW, Francois JP, Kaiser J, Prange M, Steinke T (2010) Holocene changes in the
518 position and intensity of the southern westerly wind belt. *Nat Geosci* 3:695-699

519 Lewis AR, Ashworth AC (2016) An early to middle Miocene record of ice-sheet and landscape evolution
520 from the Friis Hills, Antarctica. *Geological Society of America Bulletin*, 128: 719-738

521 Lewis AR, Marchant DR, Ashworth AC, Hedenaes L, Hemming SR, Johnsons JV, Leng MJ, Machlus ML,
522 Newton AE, Raine JI, Willenbring JK, Williams M, Wolfe AP (2008) Mid-Miocene cooling and the
523 extinction of tundra in continental Antarctica. *Proc. Natl. Acad. Sci. U.S.A* 105: 10676-10680

524 Li R, Fan J, Xue J, Meyers PA (2017) Effects of early diagenesis on molecular distributions and carbon
525 isotopic compositions of leaf wax long chain biomarker n-alkanes: Comparison of two one-year-long
526 burial experiments. *Org Geochem* 104:8-18

527 Lisiecki LE, Raymo ME (2005) A Pliocene-Pleistocene stack of 57 globally distributed benthic $\delta^{18}\text{O}$
528 records, *Paleoceanography* 20:PA1003. doi:10.1029/2004PA001071

529 Locarnini RAM, Antonov JI, Boyer TP, Garcia HE, Baranova OK, Zweng MM, Johnson DR (2010) World
530 Ocean Atlas 2009: Volume 1: Temperature. In NOAA Atlas NESDIS 68 (ed. S. Levitus). U.S.
531 Government Printing Office, Washington D.C. p. 184

532 Marshall J, Speer K (2012) Closure of the meridional overturning circulation through Southern Ocean
533 upwelling. *Nat Geosci* 5:171-180

534 Martínez - Garcia A, Rosell - Melé A, Geibert W, Gersonde R, Masqué P, Gaspari V, Barbante C (2009)
535 Links between iron supply, marine productivity, sea surface temperature, and CO_2 over the last 1.1
536 Ma. *Paleoceanography* 24:PA1207. <https://doi.org/10.1029/2008PA001657>

537 Martinez-Garcia A, Rosell-Melé A, Jaccard SL, Geibert W, Sigman DM, Haug GH (2011) Southern Ocean
538 dust-climate coupling over the past four million years. *Nature* 476:312-315

539 Matsumoto GI, Honda E, Sonoda K, Yamamoto S, Takemura T (2010) Geochemical features and sources
540 of hydrocarbons and fatty acids in soils from the McMurdo Dry Valleys in the Antarctic. *Polar*
541 *Sci* 4:187-196

542 Meyers PA, Ishiwatari R (1993) Lacustrine organic geochemistry—an overview of indicators of organic
543 matter sources and diagenesis in lake sediments. *Org Geochem* 20:867-900

544 Naraoka H, Ishiwatari R (2000) Molecular and isotopic abundances of long-chain n-fatty acids in open
545 marine sediments of the western North Pacific. *Chem. Geol* 165:23-36

546 Neff PD, Bertler NAN (2015) Trajectory modeling of modern dust transport to the Southern Ocean and
547 Antarctica. *J. Geophys. Res. Atmos* 120: 9303–9322

548 Nylen TH, Fountain AG, Doran PT (2004) Climatology of katabatic winds in the McMurdo dry valleys,
549 southern Victoria Land, Antarctica. *J Geophys Res: Atmos* 109:D03114.

550 <https://doi.org/10.1029/2003JD003937>

551 Ohkouchi N., Kawamura K., Takemoto N., Ikehara M. & Nakatsuka T. 2000. Implications of carbon
552 isotope ratios of C₂₇ - C₃₃ alkanes and C₃₇ alkenes for the sources of organic matter in the Southern
553 Ocean surface sediments. *Geophys Res Lett* 27:233-236

554 Pahnke K, Zahn R (2005) Southern Hemisphere water mass conversion linked with North Atlantic climate
555 variability. *Science* 307:1741-1746

556 Poynter J, Eglinton G (1990) Molecular composition of three sediments from Hole 717C: the Bengal Fan.
557 In: Cochran, J.R., Stow, D.A.V., et al. (Eds.), *Proceedings of Ocean Drilling Program, Scientific*
558 *Results*, vol. 166. College Station, TX (Ocean Drilling Program), pp. 155–161

559 Prah FG, Muehlhausen LA, Zahnle DL (1988) Further evaluation of long-chain alkenones as indicators of
560 paleoceanographic conditions. *Geochim Cosmochim Acta* 52:2303-2310

561 Prah FG, Wakeham SG (1987) Calibration of unsaturation patterns in long-chain ketone compositions for
562 palaeotemperature assessment. *Nature* 330:367-369

563 Rosell-Melé A, Carter J, Eglinton G (1994) Distributions of long-chain alkenones and alkyl alkenoates in
564 marine surface sediments from the North East Atlantic. *Org Geochem* 22:501-509

565 Rosell-Melé A, Eglinton G, Pflaumann U, Sarnthein M (1995) Atlantic core-top calibration of the U^K₃₇
566 index as a sea-surface palaeotemperature indicator. *Geochim Cosmochim Acta* 59:3099-3107

567 Shevenell AE, Ingalls AE, Domack EW, Kelly C (2011) Holocene Southern Ocean surface temperature
568 variability west of the Antarctic Peninsula. *Nature* 470:250-254

569 Sicre MA, Bard E, Ezat U, Rostek F (2002) Alkenone distributions in the North Atlantic and Nordic sea
570 surface waters. *Geochem Geophys Geosyst* 3. <https://doi.org/10.1029/2001GC000159>

571 Sikes EL, Sicre MA (2002) Relationship of the tetra - unsaturated C₃₇ alkenone to salinity and temperature:
572 Implications for paleoproxy applications. *Geochem Geophys Geosyst* 3.
573 <https://doi.org/10.1029/2001GC000159>

574 Sikes EL, Volkman JK (1993) Calibration of alkenone unsaturation ratios (U^{K'}₃₇) for paleotemperature
575 estimation in cold polar waters. *Geochim Cosmochim Acta* 57:1883-1889

576 Sikes EL, Volkman JK, Robertson LG, Pichon JJ (1997) Alkenones and alkenes in surface waters and
577 sediments of the Southern Ocean: Implications for paleotemperature estimation in polar
578 regions. *Geochim Cosmochim Acta* 61:1495-1505

579 Theissen KM, Dunbar RB, Cooper AK, Mucciarone DA, Hoffmann D (2003) The Pleistocene evolution of
580 the East Antarctic Ice Sheet in the Prydz Bay region: stable isotopic evidence from ODP Site
581 1167. *Global and Planetary Change* 39:227-256

582 Thomas EK, Huang Y, Morrill C, Zhao J, Wegener P, Clemens SC, Colman SM, Gao L (2014) Abundant

583 C₄ plants on the Tibetan Plateau during the late glacial and early Holocene. *Quat Sci Rev* 87:24–33
584 Tiedemann R (2012) FS Sonne Fahrtbericht/Cruise Report SO213. Alfred Wegener Institute,
585 Bremerhaven.

586 Toggweiler JR, Russell J (2008) Ocean circulation in a warming climate. *Nature* 451:286-288

587 Toyos MH, Lamy F, Lange CB, Lembke-Jene L, Saavedra-Pellitero M, Esper O, Arz HW (2020) Antarctic
588 circumpolar current dynamics at the Pacific entrance to the Drake Passage over the past 1.3
589 million years. *Paleoceanography and Paleoclimatology* 35:e2019PA003773.
590 <https://doi.org/10.1029/2019PA003773>

591 Venkatesan MI (1988) Organic geochemistry of marine sediments in Antarctic region: Marine lipids in
592 McMurdo Sound. *Org Geochem* 12:13-27

593 Vogts A, Moossen H, Rommerskirchen F, Rullkötter J (2009) Distribution patterns and stable carbon
594 isotopic composition of alkanes and alkan-1-ols from plant waxes of African rain forest and savanna
595 C₃ species. *Org Geochem* 40:1037-1054

596 Volkman JK, Barrett SM, Blackburn SI, Mansour MP, Sikes EL, Gelin F (1998) Microalgal biomarkers: a
597 review of recent research developments. *Org Geochem* 29:1163-1179

598 Wu Li, Wang Rujian, Xiao Wenshen, Ge Shulan, Chen Zhihua (2015) High resolution age model of Late
599 Quaternary Mouth Fan at Prydz Trough, Eastern Antarctic. *Marine Geology and Quaternary Geology*
600 (in Chinese with English abstract) 35:197-208

601 Yamamoto M, Shiraiwa Y, Inouye I (2000) Physiological responses of lipids in *Emiliana huxleyi* and
602 *Gephyrocapsa oceanica* (Haptophyceae) to growth status and their implications for alkenone
603 paleothermometry. *Org Geochem* 31:799-811

604 Zech M, Pedentchouk N, Buggle B, Leiber K, Kalbitz K, Marković SB, Glaser B (2011) Effect of leaf
605 litter degradation and seasonality on D/H isotope ratios of n-alkane biomarkers. *Geochim Cosmochim*
606 *Acta* 75:4917-4928

607

608 Table 1 Concentrations, $\delta^{13}\text{C}$ values and typical indices based on *n*-alkanes in the subsamples with
 609 different sediment depth. The relative contribution of long chain *n*-alkanes from C₃ and C₄ plants are
 610 calculated by carbon isotopes of the C₃₁ *n*-alkane.

Depth (cm)	$\delta^{13}\text{C}_{23}$ (‰)	$\delta^{13}\text{C}_{24}$ (‰)	$\delta^{13}\text{C}_{25}$ (‰)	$\delta^{13}\text{C}_{26}$ (‰)	$\delta^{13}\text{C}_{27}$ (‰)	$\delta^{13}\text{C}_{28}$ (‰)	$\delta^{13}\text{C}_{29}$ (‰)	$\delta^{13}\text{C}_{31}$ (‰)	<i>n</i> -alkanes ^a (ng/g)	C ₄ (%)	C ₃ (%)	ACL ^b	CPI ^c
16	-29.6	-28.8	-29.9	-33.2	-28.5	-32.2	-27.4	-28.3	445	55	45	30.1	1.6
88	-29.5	-31.8	-27.3	-30.0	-26.3	-33.1	-25.1	-25.5	328	75	25	30.3	2.0
166	-25.4	-26.4	-26.7	-32.5	-28.3	-38.0	-27.1	-27.8	295	59	41	30.1	2.1
243	-27.1	-26.8	-26.8	-30.4	-26.7	-33.3	-29.8	-28.3	362	55	45	30.3	2.5
323	-29.8	-31.2	-30.6	-35.0	-28.3	-32.1	-29.4	-27.9	324	58	42	29.3	1.3
398	-31.5	-35.9	-30.0	-36.7	-28.6	-34.6	-25.0	-24.8	787	80	20	29.6	1.3
482	-26.8	-28.4	-29.3	-30.3	-26.8	-30.1	-27.4	-26.6	411	67	33	30.7	1.9
550	-27.1	-30.7	-29.3	-35.1	-27.8	-31.2	-27.8	-25.4	420	76	24	30.1	1.6
626	-30.4	-32.2	-31.7	-34.6	-29.6	-30.9	-26.4	-25.8	344	73	27	29.6	1.6
698	-28.6	-30.6	-29.0	-32.7	-27.8	-31.8	-27.0	-25.8	490	73	27	29.3	1.1
762	-28.8	-29.3	-30.0	-35.3	-26.7	-32.1	-30.4	-29.4	455	47	53	29.8	1.6
818	-28.8	-28.7	-32.3	-37.4	-30.1	-35.8	-27.7	-27.2	503	63	37	30.1	1.7

611

612 a: Total concentrations of C₂₃-C₃₅ *n*-alkanes

613 b: $\text{ACL}_{27-35} = \sum(i \times X_i) / \sum X_i$, where X is abundance and i ranges from C₂₇-C₃₅ odd *n*-alkanes

614 c: $\text{CPI}_{27-33} = 0.5 \times \sum(\text{C}_{27}-\text{C}_{33}) / (\text{C}_{26}-\text{C}_{32}) + 0.5 \times \sum(\text{C}_{27}-\text{C}_{33}) / (\text{C}_{28}-\text{C}_{34})$

615

616 Table 2 The relative abundance and concentrations of C_{37:4}, C_{37:3} and C_{37:2} alkenones and based on U₃₇^k-
 617 and U₃₇^{k'}-SST in the subsamples with different sediment depth.

Depth (cm)	C _{37:4} (%)	C _{37:3} (%)	C _{37:2} (%)	Alkenones (ng/g)	U ₃₇ ^k -SST ^a (°C)	U ₃₇ ^{k'} -SST ^b (°C)
16	12	85	4	90.7	0.6	-0.1
88	11	87	3	104.2	0.7	-0.4
166	30	40	30	13.2	2.8	11.5
243	21	51	28	15.3	4.4	9.2
323	35	48	17	14.7	-1.7	6.6
398	16	64	19	50.1	3.5	5.6
482	15	80	6	65.1	0.5	0.7
550	37	38	24	12.6	-0.6	10.3
626	30	44	26	14.0	1.8	9.9
698	23	59	18	19.1	1.2	5.7
762	25	27	48	30.2	8.4	17.9
818	30	36	34	19.0	3.6	13.2

618

619 a: $U_{37}^{k'} = C_{37:2} / (C_{37:2} + C_{37:3})$

620 b: $U_{37}^k = (C_{37:2} - C_{37:4}) / (C_{37:2} + C_{37:3} + C_{37:4})$

621

622 FIGURE CAPTIONS:

623
624 Fig. 1. Map of the Southern Ocean and the continent of Antarctica. The red pentagram denotes the site of
625 the sediment core in our study. Red triangles indicate sites of sea surface temperature or sea subsurface
626 temperature records reported in previous studies. The SST record in the PS75/034-2 sediment core was
627 used for the U_{37}^k index (Ho et al., 2012), whereas other sediment cores (ODP 1098, JPC 10 and
628 MD03-2601) were used for TEX_{86} (Shevenell et al., 2011; Kim et al., 2012; Etourneau et al., 2013). The
629 thick blue line indicates the Antarctic Circumpolar Current (ACC). The solid dots denote ice core locations
630 in the Antarctic, including Dome C and Vostok.

631
632 Fig. 2. The concentrations (C_{23} - C_{35}), ACL (C_{27-35} - C_{35}) and CPI (C_{27} - C_{33}) values of *n*-alkanes at different
633 depths of the sedimentary section.

634
635 Fig. 3. The relative abundance of long chain *n*-alkanes (C_{23} - C_{35}) at different depths of the sedimentary
636 section.

637
638 Fig. 4. Relationship between ACL_{27-35} and CPI_{27-33} of long chain *n*-alkanes.

639
640 Fig. 5. The average $\delta^{13}C$ values of *n*-alkanes. Error bars represent 1 standard deviation of 12 samples.

641
642 Fig. 6. The relative abundance of $C_{37:4}$, $C_{37:3}$ and $C_{37:2}$ alkenones and the calculated sea surface
643 temperature based on U_{37}^k and $U_{37}^{k'}$ index at different depths of the sedimentary section. The light grey
644 and light blue bands represent modern average summer SST and highest SST during the Holocene at the
645 same latitude of the Southern Ocean, respectively.

646

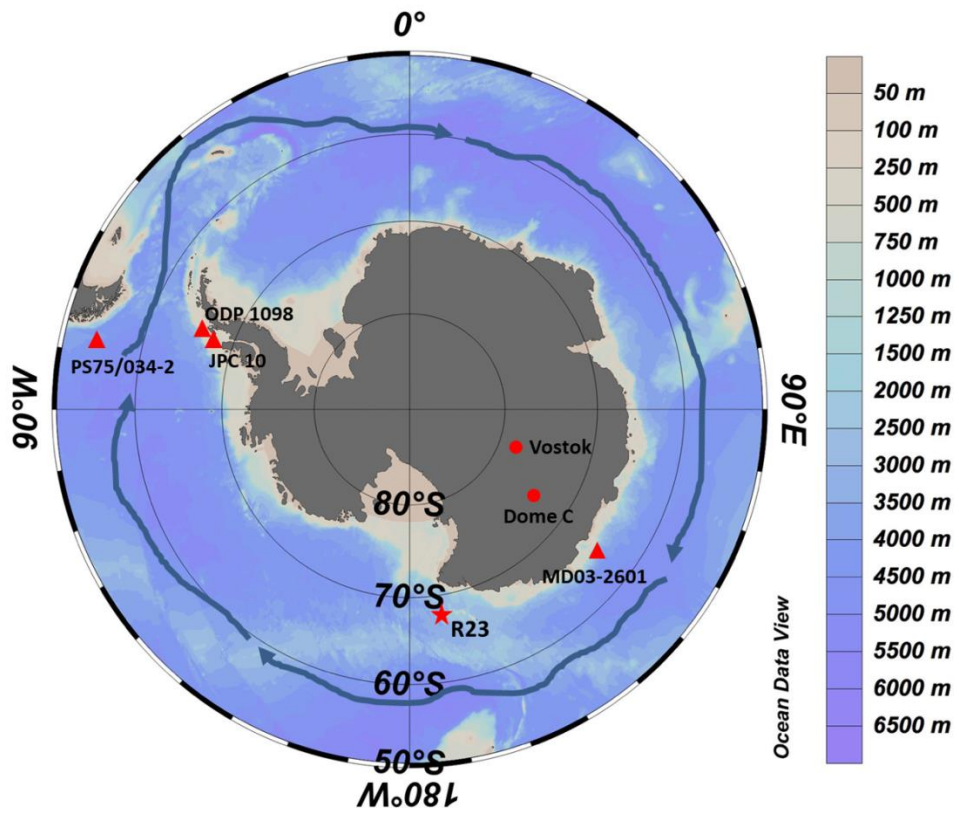


Figure 1

647
648
649
650

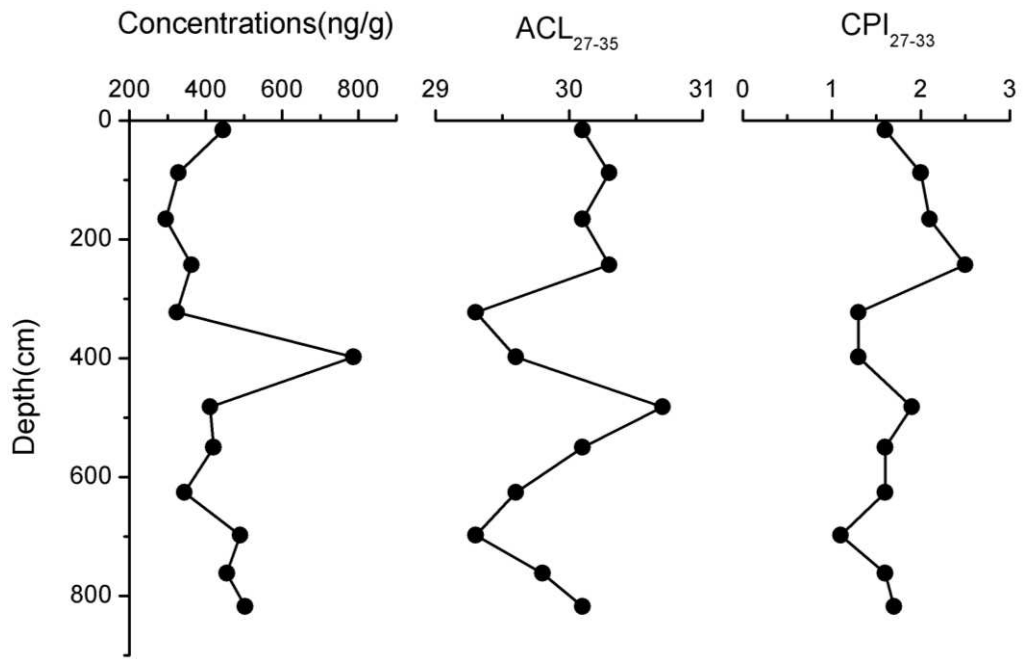


Figure 2

651
652
653
654

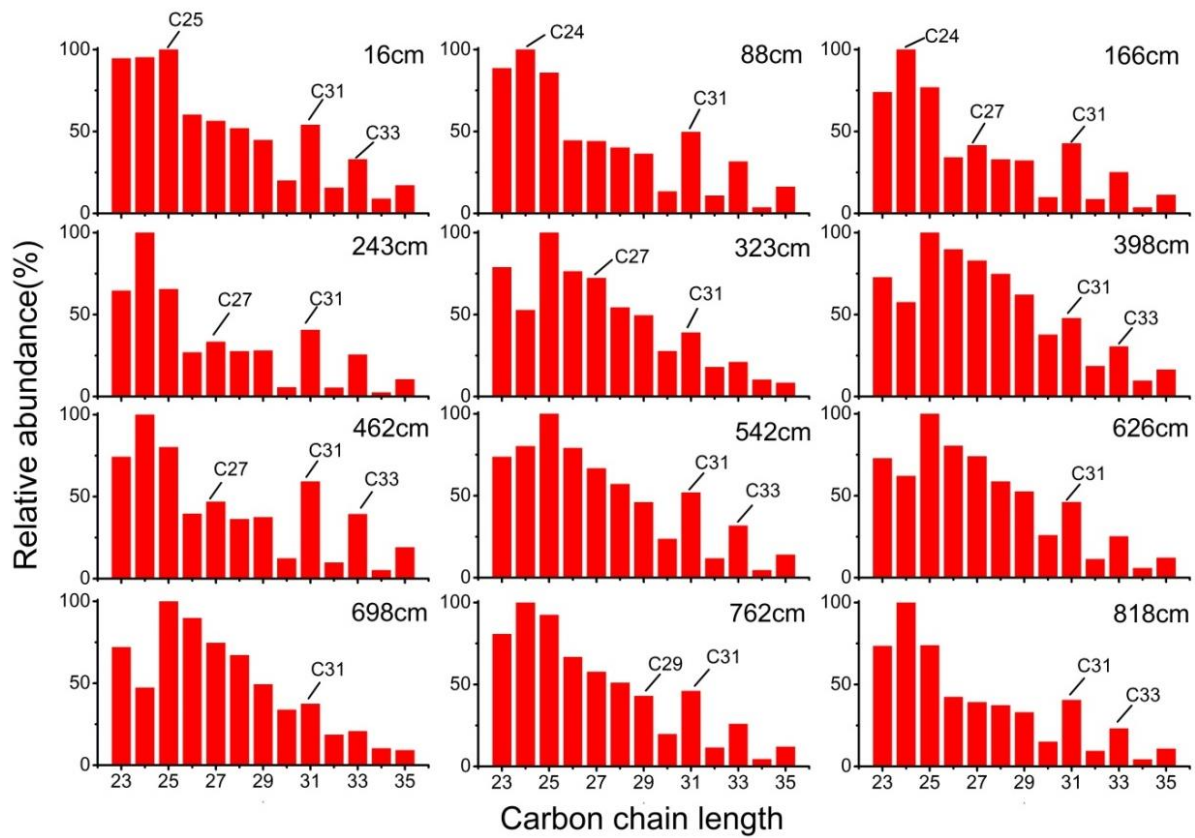
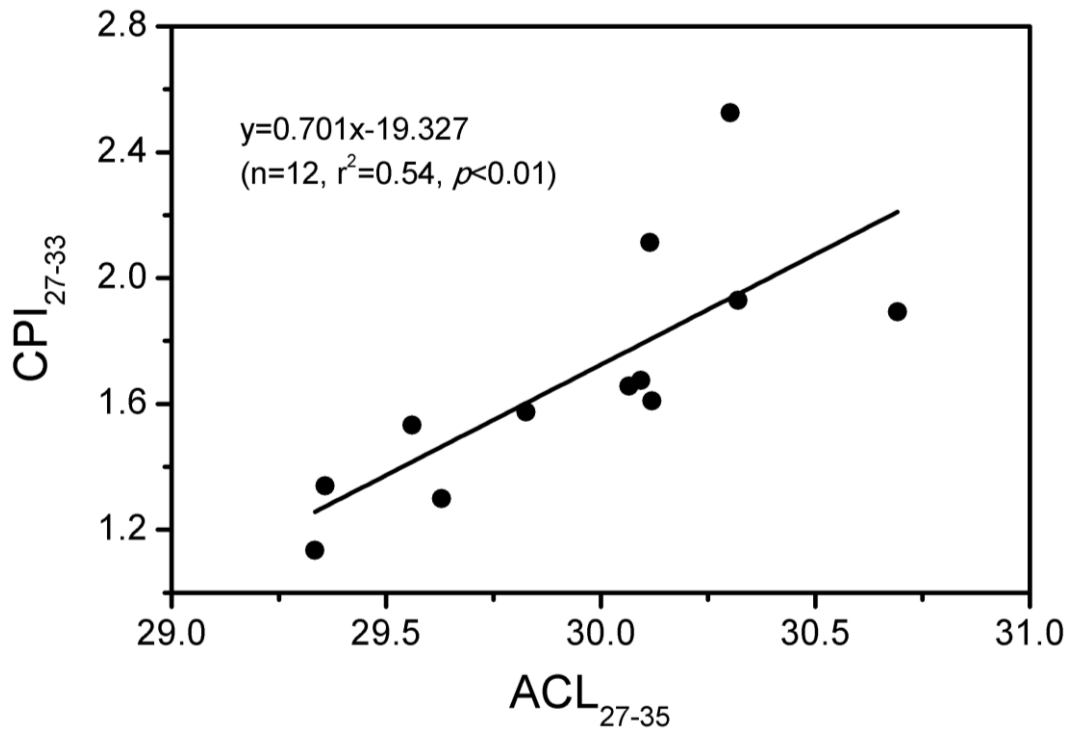


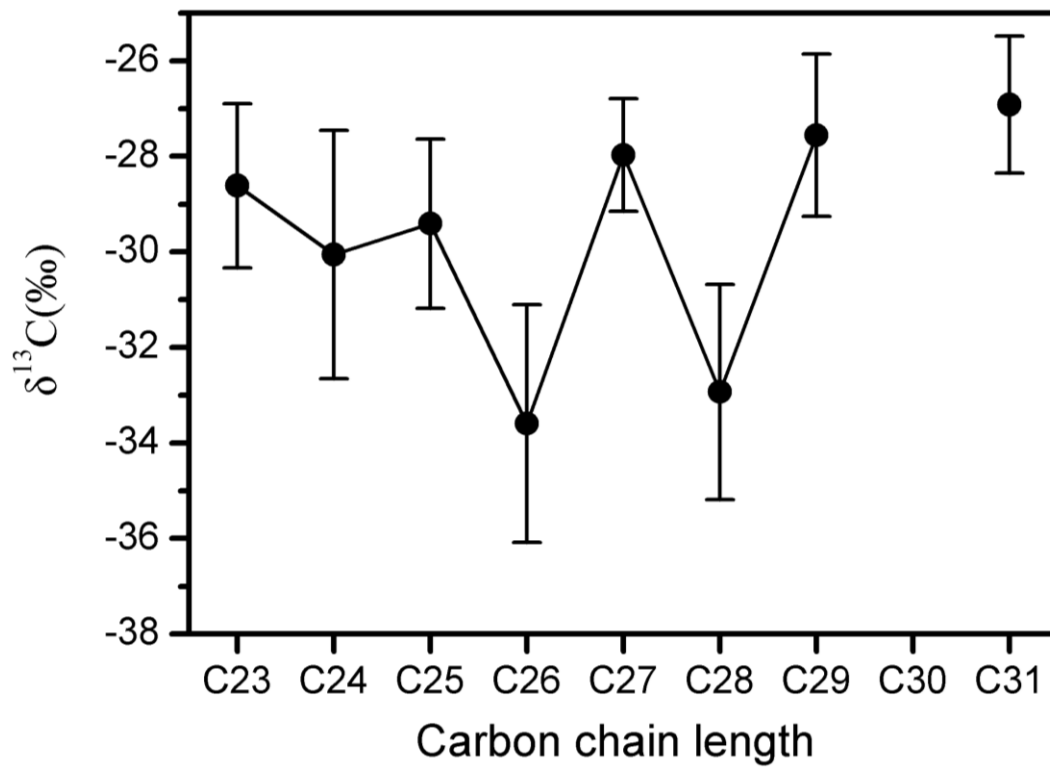
Figure 3

655
656
657
658



659
660
661
662

Figure 4



663
664
665
666

Figure 5

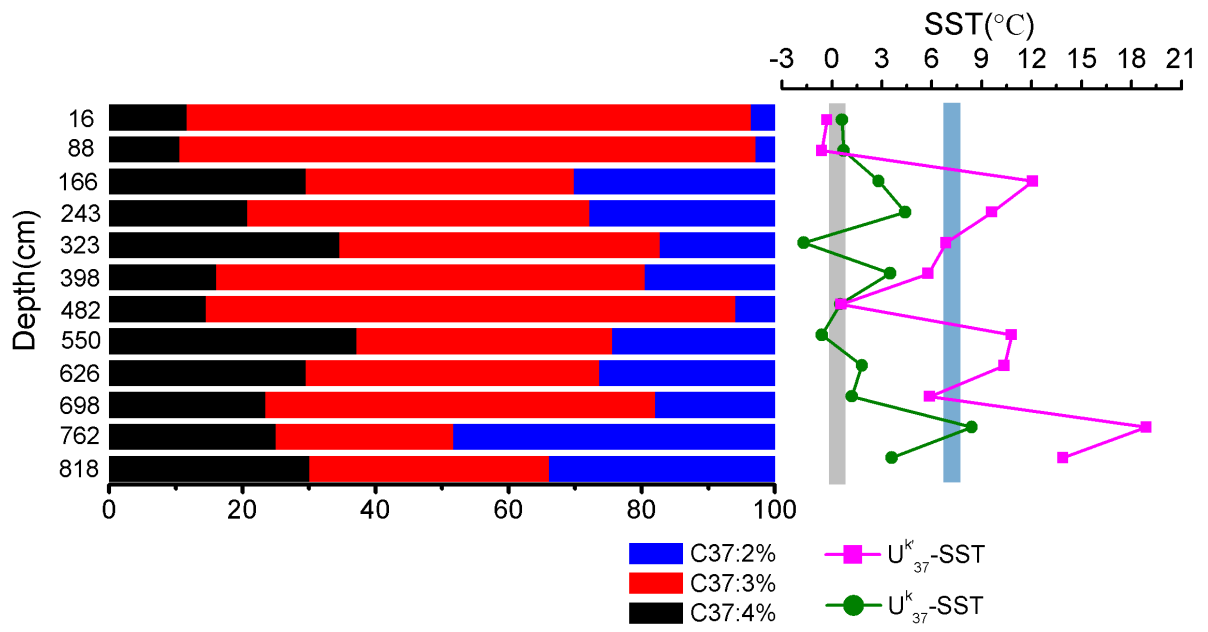


Figure 6

667

668

669

670

Figures

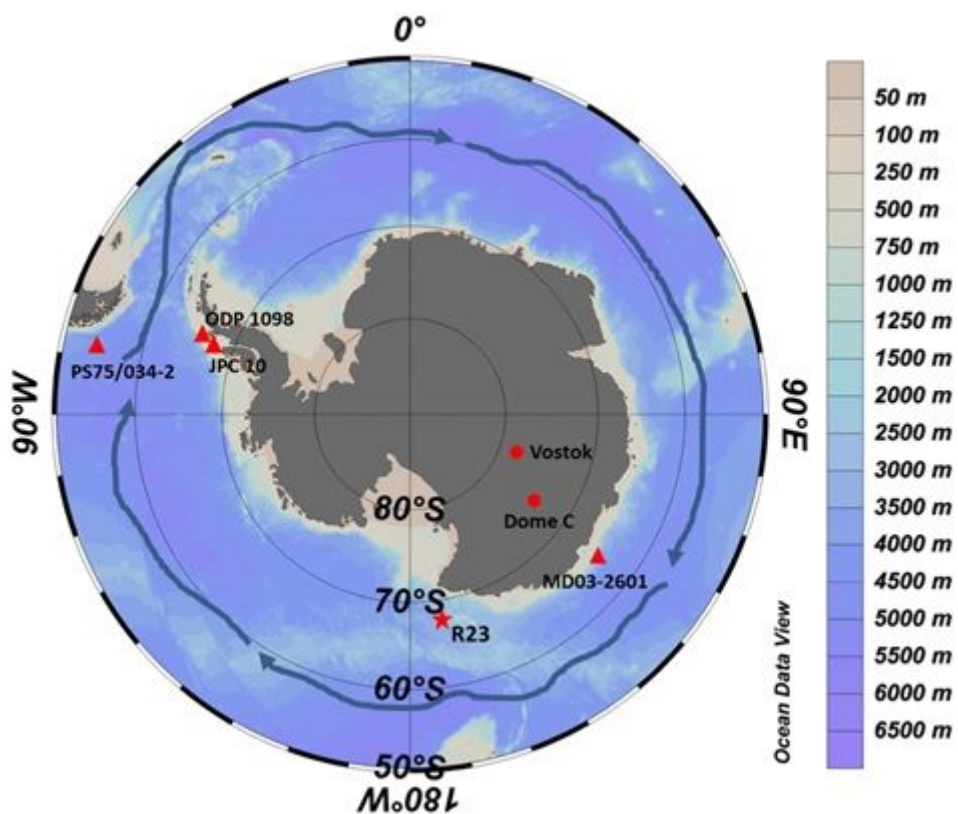


Figure 1

Map of the Southern Ocean and the continent of Antarctica. The red pentagram denotes the site of the sediment core in our study. Red triangles indicate sites of sea surface temperature or sea subsurface temperature records reported in previous studies. The SST record in the PS75/034-2 sediment core was used for the U_{37}^k index (Ho et al., 2012), whereas other sediment cores (ODP 1098, JPC 10 and MD03-2601) were used for TEX86 (Shevenell et al., 2011; Kim et al., 2012; Etourneau et al., 2013). The thick blue line indicates the Antarctic Circumpolar Current (ACC). The solid dots denote ice core locations in the Antarctic, including Dome C and Vostok.

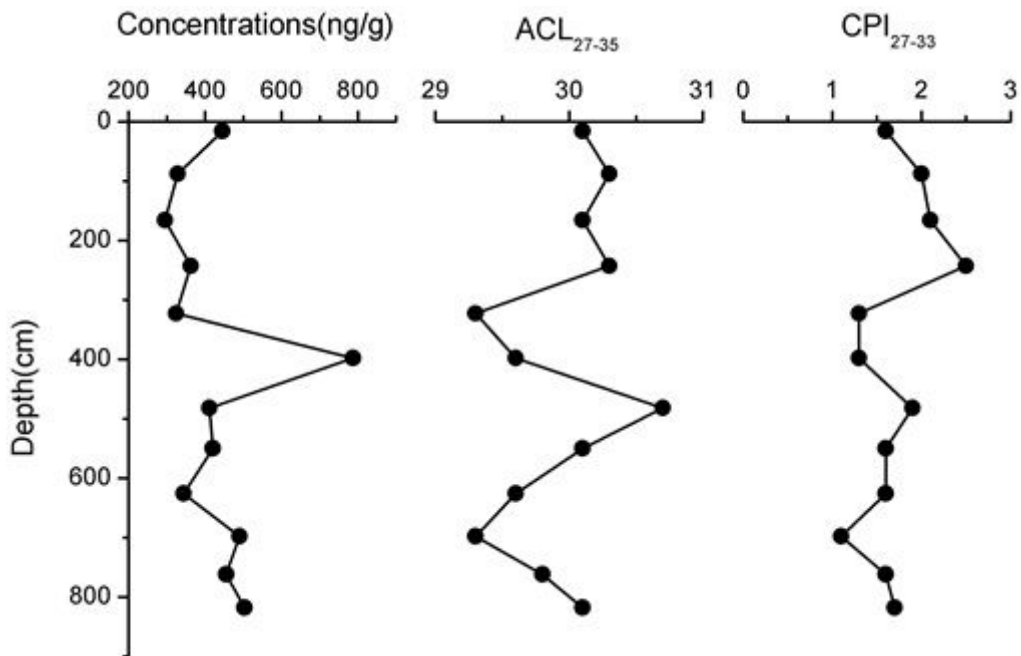


Figure 2

The concentrations (C23-C35), ACL (C27-35-C35) and CPI (C27-C33) values of n-alkanes at different depths of the sedimentary section.

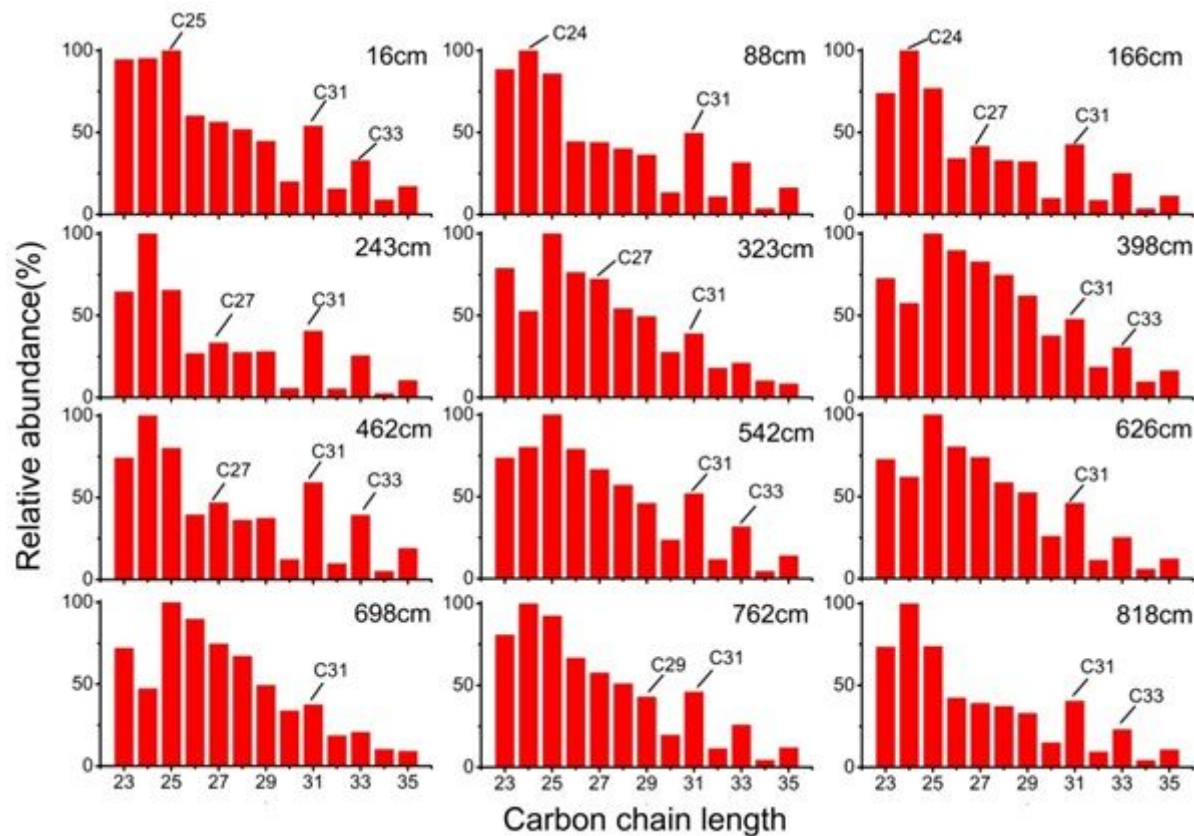


Figure 3

The relative abundance of long chain n-alkanes (C23-C35) at different depths of the sedimentary section.

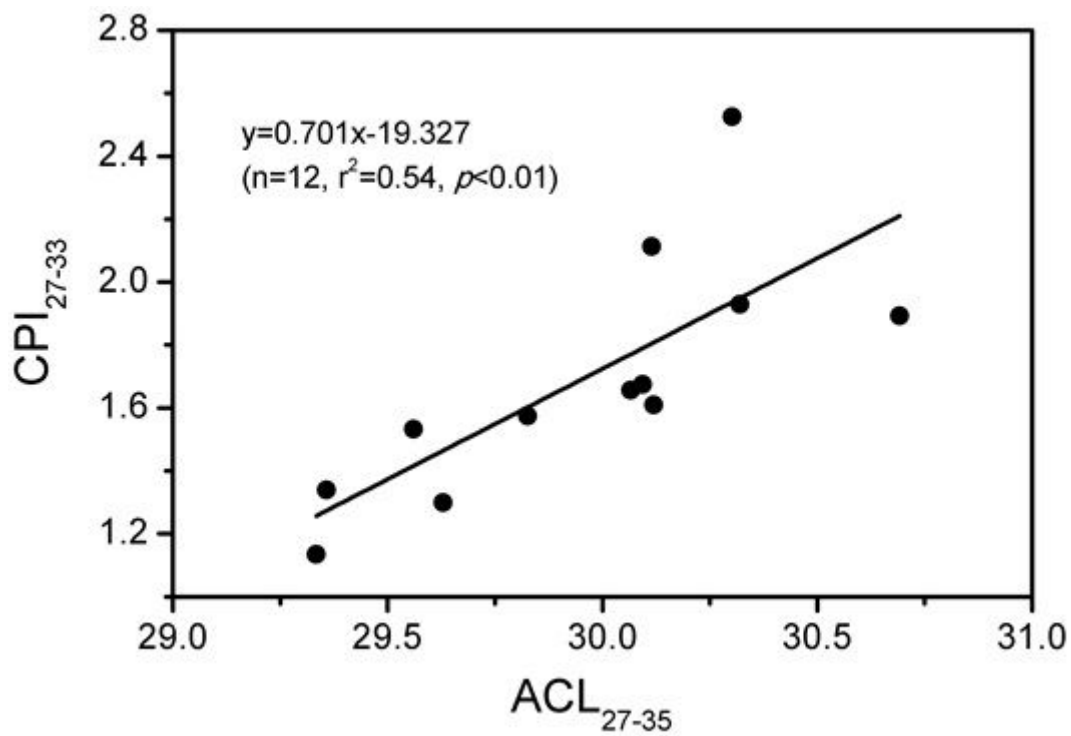


Figure 4

Relationship between ACL_{27-35} and CPI_{27-33} of long chain n-alkanes.

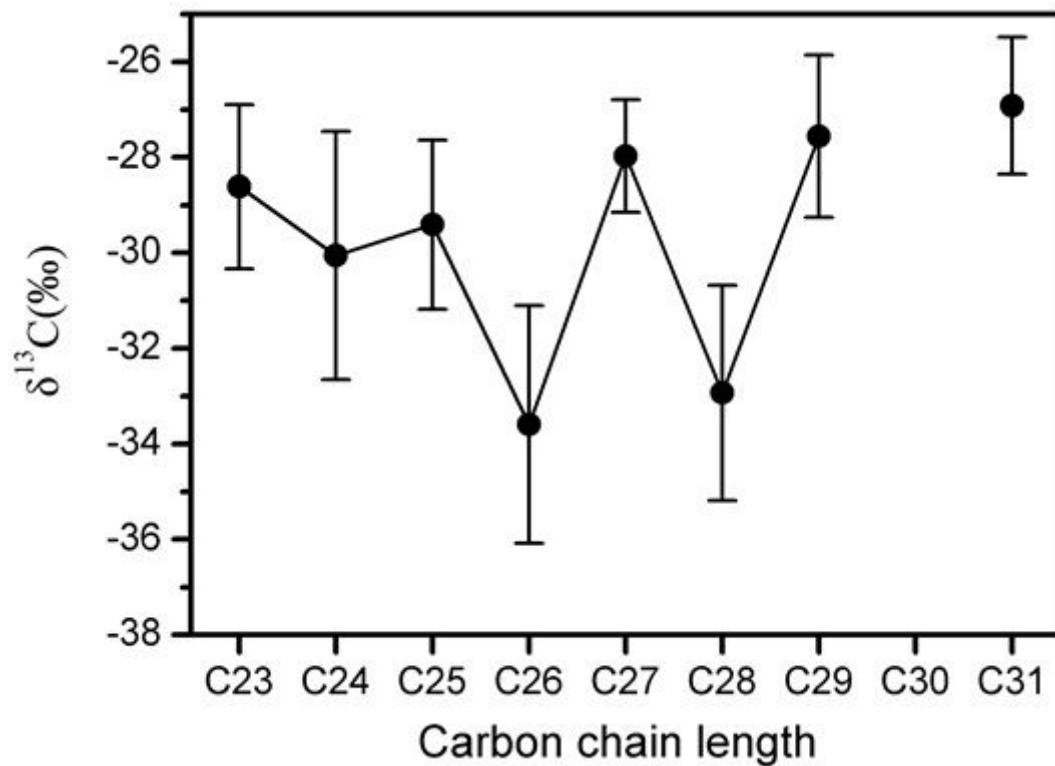


Figure 5

The average $\delta^{13}C$ values of n-alkanes. Error bars represent 1 standard deviation of 12 samples.

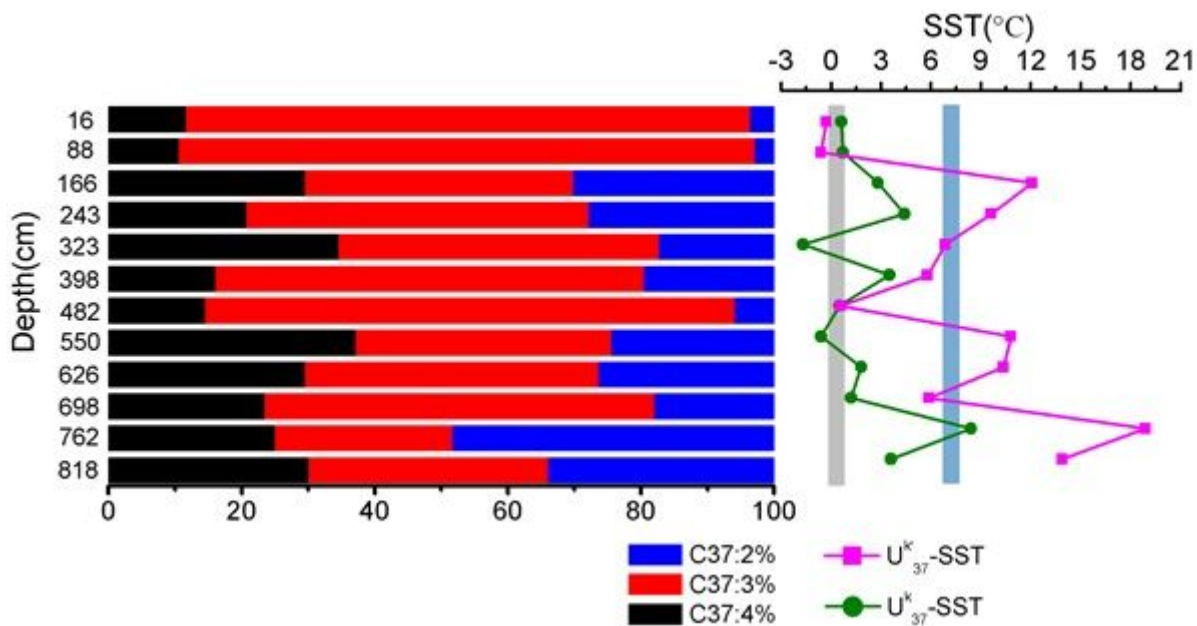


Figure 6

The relative abundance of C37:4, C37:3 and C37:2 alkenones and the calculated sea surface temperature based on U₃₇^k and U₃₇^{k'} index at different depths of the sedimentary section. The light grey and light blue bands represent modern average summer SST and highest SST during the Holocene at the same latitude of the Southern Ocean, respectively.

Supplementary Files

This is a list of supplementary files associated with this preprint. Click to download.

- [Supplementarymaterials.docx](#)